Received: 28 April 2021

DOI: 10.1002/mop.32992

WILEY

RESEARCH ARTICLE

Folded microstrip antenna with isotropic radiation pattern

Dong-Su Choi[1] | Yoon-Seon Choi[1] | Dae-Keun Ju[1] | Bang Chul Jung[2] | Jong-Myung Woo[1]

[1]Department of Radio and Information Communications Engineering, Chungnam National University, Daejeon, Republic of Korea

[2]Department of Electronics Engineering, Chungnam National University, Daejeon, Republic of Korea

Correspondence
Jong-Myung Woo, Department of Radio and Information Communications Engineering, Chungnam National University, Daejeon, Republic of Korea.
Email: jmwoo@cnu.ac.kr

Abstract

In contrast to existing antennas with polarization and directional characteristics, we propose a novel isotropic antenna that provides equivalent vertical and horizontal polarization in all directions. The final design was guided by simulations, with the performance characteristics of the fabricated antenna verified experimentally. In the proposed antenna, two $\lambda/4$ folded microstrip antennas were integrated into one antenna in a "+" shape to generate the isotropic radiation pattern, with the input impedance matched to the feeding position. The resonant frequency, horizontal width, radiation pattern, and axis ratio were adjusted by changing the length of the microstrip line. Both simulations and experiments confirmed that the radiation patterns of vertical and horizontal polarization on each plane show the characteristics of an isotropic antenna with nondirectional radiation pattern.

KEYWORDS

folded microstrip antenna, isotropic antenna, nondirectional radiation pattern, vertical and horizontal polarization

1 | INTRODUCTION

Polarization and directivity were fundamental properties in all types of antennas. For instantce, microstrip antenna and horn antenna have directivity. Due to existence of polarization, isotropic antenna that has equal vertical and horizontal polarization components in all directions has been known almost impossible to be implemented in practice. Nevertheless, if an antenna exhibiting an isotropic pattern for both vertical and horizontal polarization can be developed, it will be effective as a standard antenna.

In this article, we present a novel design of folded microstrip linearly-polarized antenna with a nondirectional pattern in the E-plane and an elliptical pattern in the H-plane. Based on this, the two antennas were combined into a "+" shape. This letter proposes a design for an isotropic antenna in which the E-plane and H-plane radiation patterns for both vertical and horizontal were nondirectional in all directions.

2 | ANTENNA DESIGN

2.1 | $\lambda/2$ microstrip antenna

The basic $\lambda/2$ (λ: wavelength) microstrip patch antenna structure and electric field were shown in Figure 1(A). The radiating element length L was $\lambda/2$, and the width W can also be set close to $\lambda/2$.[1–3] In addition, h represents the height of the patch, and the resonance mode was set TM^{z}_{100} in the cavity model. On the top view, the leakage electric field distribution corresponding to the case where the ground plane was larger than the radiating element was shown, as can be seen in Figure 1(B), for which the leakage electric field length ΔL was assumed to be similar to the height of the patch. Here, since the field distribution of the vertical polarization is in phase, it contributes to the radiation. However, since the field distribution of the horizontal polarization is out of phase in TM^{z}_{100} mode, it does not contribute to radiation.

We performed simulations for the antenna in Figure 2(A) with the center frequency 118 MHz (λ: 2542 mm) of the ground-based augmentation system.[4,5] The simulation and characteristic analysis of the antenna was performed using the MWS analysis software(CST, 2017). Probe feeding was used for the feeding mechanism, and styrofoam was selected as a dielectric material with air-like properties. The design dimensions and characteristics were shown in Figure 2. The ground plane size was set to $1\lambda \times 1\lambda$. The S_{11} parameter was −16.7 dB, and the radiation pattern of the signal polarized paralleled to the x-axis. In the case of the y-axis parallel polarization, not only leakage electric field was out of phase, but also the feed

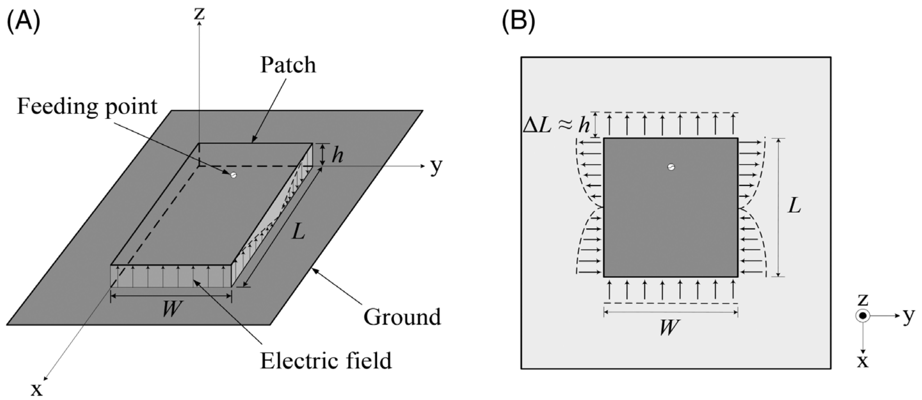

FIGURE 1 Schematic illustrations of the $\lambda/2$ microstrip antenna structure and TM^z_{100} mode: (A) Structure; (B) Top view and leakage electric field

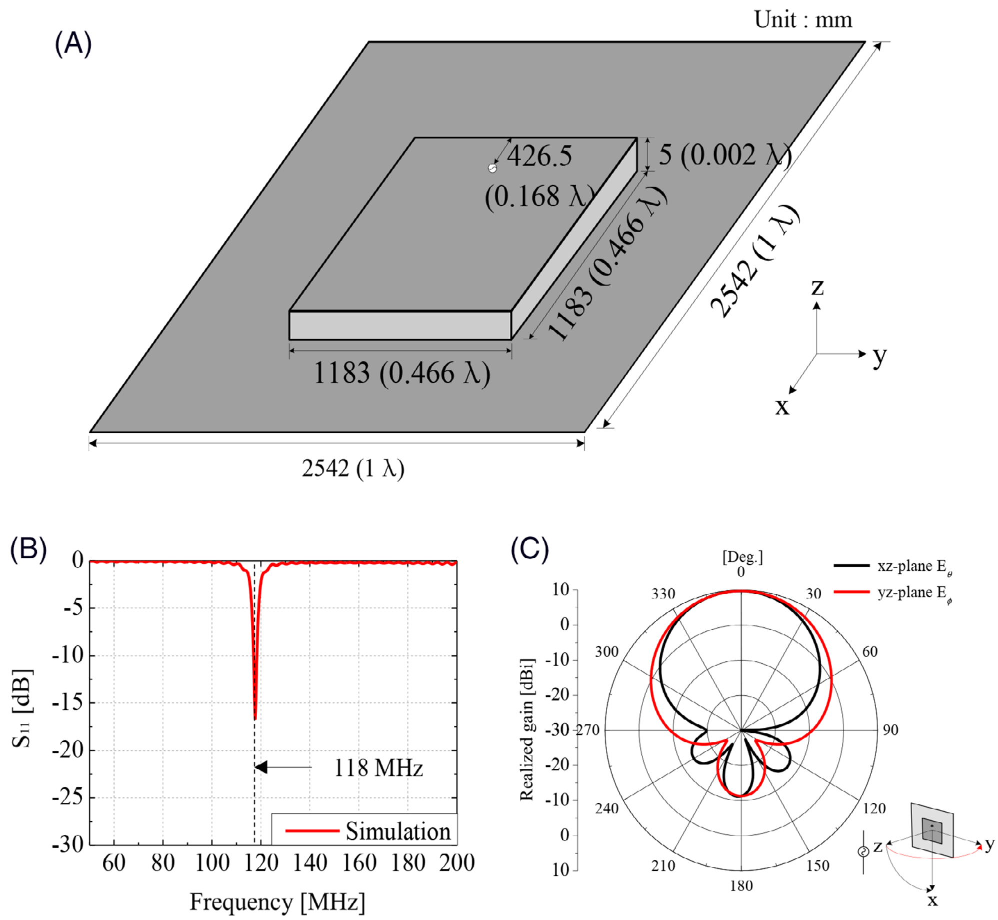

FIGURE 2 Design parameters of the $\lambda/2$ microstrip antenna: (A) Structure; (B) S_{11}; (C) Radiation pattern [Color figure can be viewed at wileyonlinelibrary.com]

point was located at the center of the horizontal axis (*y*-axis), which renders impedance matching impossible and results in a large return loss. Therefore, the radiation output comprises the vertical polarization contribution only, and it was difficult to obtain a horizontal polarization radiation pattern.

2.2 | $\lambda/4$ folded microstrip antenna

To extract an effective radiation contribution from the horizontal polarization, the *x*-axis antenna length *L* was folded, thus becoming $\lambda/4$, as shown in Figure 3(A).[6–10] In addition, the size of the ground plane was designed to be equal to the

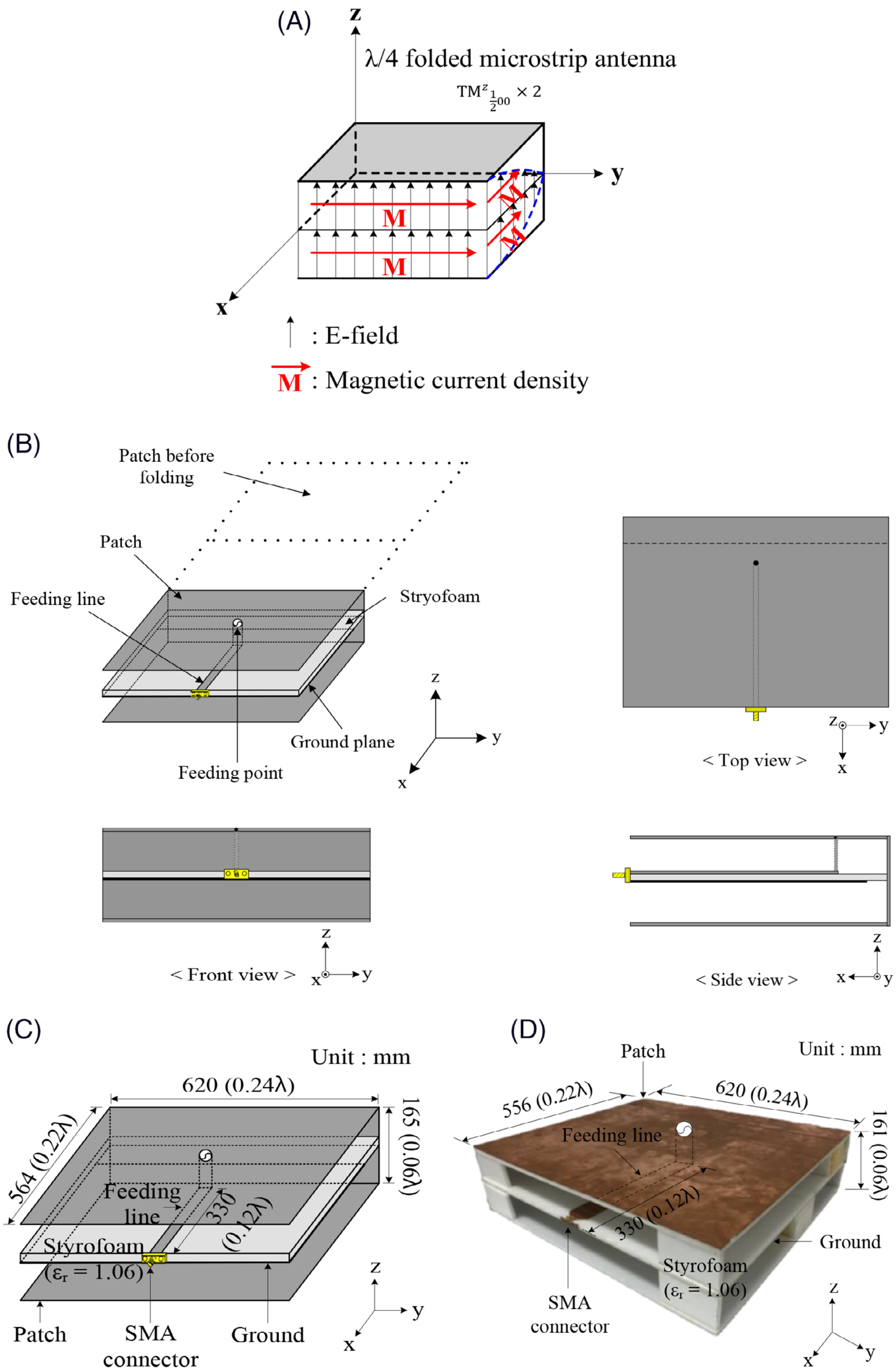

FIGURE 3 Configuration schematic illustration and fabrication of the $\lambda/4$ folded microstrip antenna mode and design characteristics: (A) $\lambda/4$ folded microstrip antenna mode; (B) Schematic of $\lambda/4$ folded microstrip antenna; (C) Simulation structure; (D) Fabricated structure; (E) S_{11}; (F) Radiation pattern [Color figure can be viewed at wileyonlinelibrary.com]

size of the radiating element. Accordingly, the magnetic current density **M** on the aperture surface becomes in-phase, and the electric field distribution on the *x*-axis contributes to radiation even in the *xy*-plane. The schematic of the $\lambda/4$ folded microstrip antenna was shown in Figure 3(B). The actual feeding was transformed into a structure in which

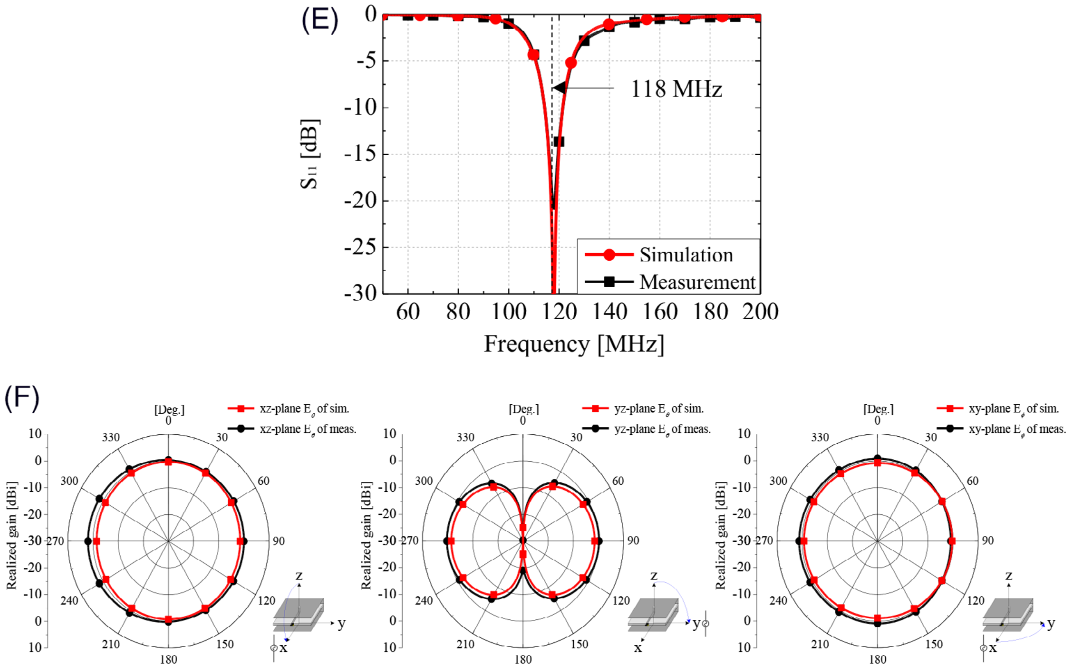

FIGURE 3 Continued [Color figure can be viewed at wileyonlinelibrary.com]

the ground plane and the microstrip line were inserted centrally, as shown in Figure 3(C). The simulation yielded a S_{11} value of −36.13 dB. The E_θ component (E-plane) was nondirectional in the *xz*-plane. In addition, the E_θ component (H-plane) formed a radiation pattern with a difference of 1.38 dB between the maximum and the minimum level in the *xy*-plane. The reason the level was low in the $\pm x$-axis direction was that the electric field distribution has a sine distribution. However, This level difference can be overcome by adjusting the opening width of the *yz*-plane. The E_θ component shows a directional pattern in the *yz*-plane from the polarization effect.

The fabricated antenna were shown in Figure 3(D). In this case, S_{11} was measured as −22.36 dB, and the radiation pattern was consistent with the simulation result. From these results, if such antennas were properly coupled, the directional pattern of E_θ components in the *yz*-plane becomes possible as a nondirectional pattern. It also creates a nondirectional pattern of the E_ϕ component in the *xz*-plane. Then, the challenge to obtain an isotropic pattern in all directions for the vertical and horizontal polarization remained.

3 | PROPOSED MICROSTRIP ANTENNA

First, as shown in Figure 4(A), two $\lambda/4$ folded microstrip antennas were combined in a "+" shape to obtain an isotropic electric field distribution. Next, the microstrip line was placed near the intersection at which the antennas were orthogonally combined to each other. Two resonant frequencies by the difference in the antenna width were obtained. Then, using the difference in feed impedance of each antenna, the phase difference was designed to be 90° from the center frequency. The data results for this were shown in Figure 4(C), yielding a S_{11} value of −13.43 dB at the center frequency of 118 MHz. In addition, circular polarization was generated in the $\pm x$-axis direction, with the E_θ and E_ϕ components representing the vertical and horizontal polarizations, respectively, providing nondirectionality in the *xz*-, *yz*-, and *xy*-planes. In the *xz*-plane, the difference between the maximum and minimum levels of the E_θ and E_ϕ components was 2.61 and 1.13 dB, respectively.

The fabricated antenna were shown in Figure 4(B). With several tunnings final dimensions of the antenna was conformed. After this, the S_{11} characteristics associated with the dimensional change of the fabricated antenna parameters were measured. In response to varying the width P_w, it was confirmed that the resonant frequency increased owing to the effect of the antenna length decreasing as P_w became shorter. As a result, when P_w was 295 mm, that is, 37 mm shorter than the simulation length, resonance characteristics were exhibited at the center frequency of 118 MHz. In addition, the microstrip line length F_l affects the input impedance, with a F_l of 475 mm providing good circular polarization characteristics in the $\pm x$-axis. In the given dimension, S_{11} was measured as −10.4 dB at the center frequency of 118 MHz. In the same way as in the simulation, in *xz*-, *yz*-, and *xy*-plane, both and E_ϕ

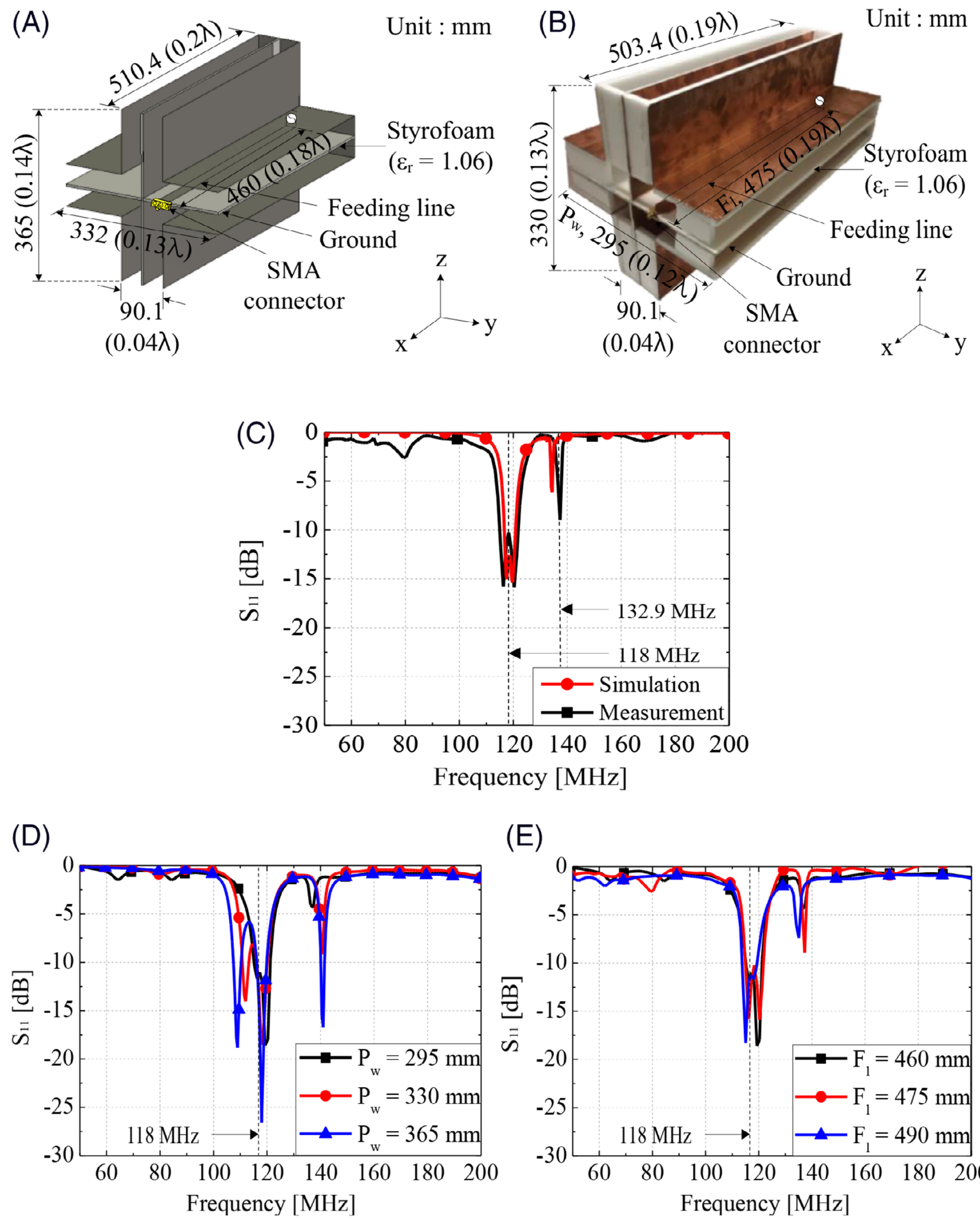

FIGURE 4 Configuration schematic illustration and fabrication of the proposed microstrip antenna mode and design characteristics: (A) Simulation structure; (B) Fabricated structure; (C) S_{11}; (P_w: 295 mm, F_l: 475 mm); (D) Change of S_{11} according to P_w length; (E) Change in S_{11} according to F_l length; (F) Radiation pattern (P_w: 295 mm, F_l: 475 mm); (G) 3D radiation pattern [Color figure can be viewed at wileyonlinelibrary.com]

showed nondirectional patterns. The results were shown in Table 1. In Figure 4(F), it was confirmed that the radiation field was isotropic by adjusting scale of the radiation pattern. In addition, the 3D radiation pattern was shown to be an isotropic pattern in Figure 4(G).

On the other hand, in the resonance characteristic at 132.9 MHz, the feed point was shown as a $+y$-axis offset from the center, and the E_θ component of the yz-plane (1/4 plane) formed by the $+y$-axis length and the $+z$-axis length makes a pattern.

Figure 5 was shown the axial ratio in the $\pm x$ axis. The axial ratio was designed to produce right-handed circular polarization in the $+x$ axis, and the magnitude was measured as 0.75 dB. As a result of left-handed circular polarization, the axial ratio measured in the $-x$-axis was 0.91 dB, indicating good circular polarization characteristics.

4 | CONCLUSION

In this letter, an isotropic antenna capable of emitting vertical and horizontal polarization simultaneously in all directions was designed. To make an isotropic radiation pattern, first, by folding the $\lambda/2$ microstrip antenna, the side current

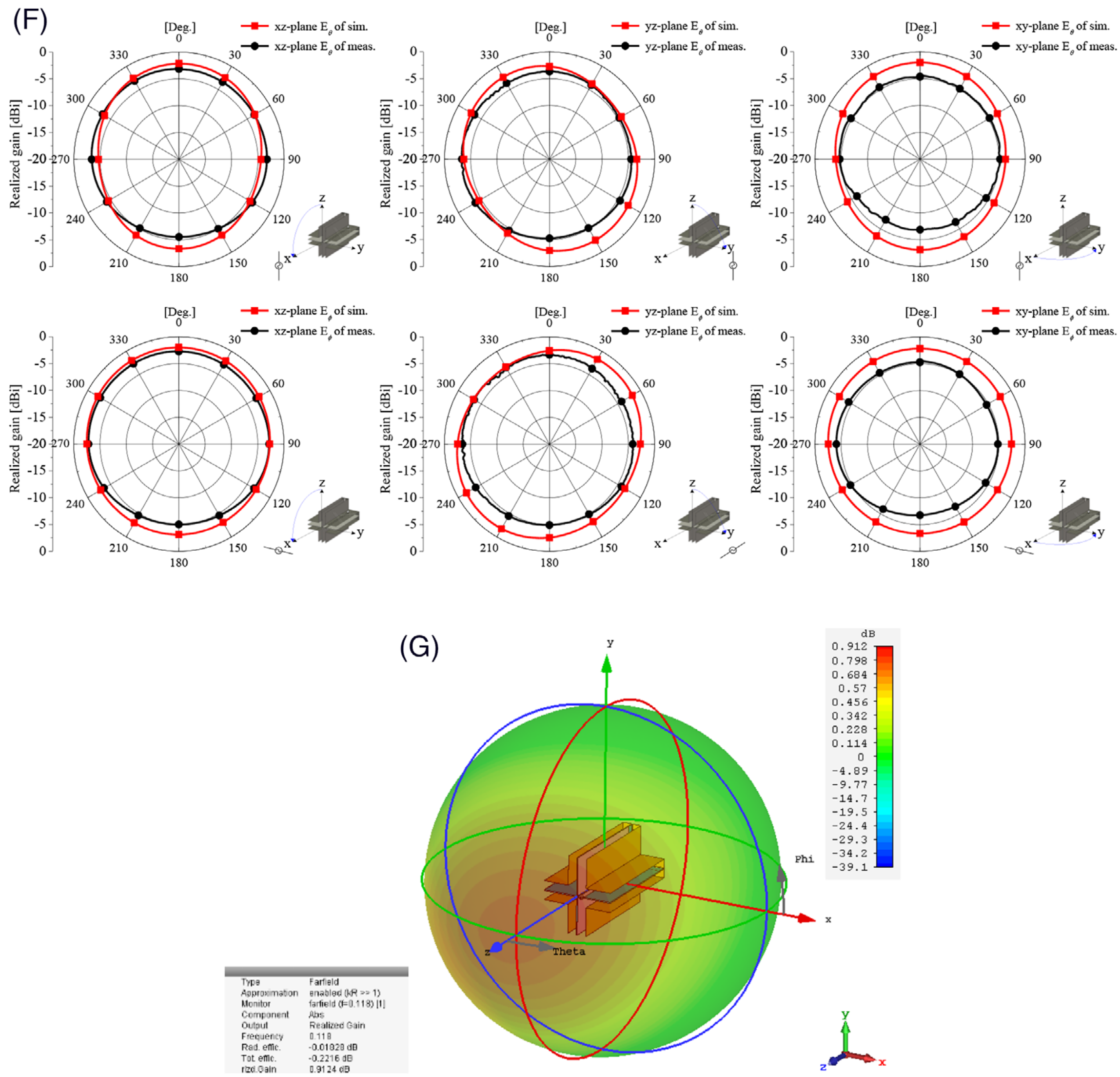

FIGURE 4 Continued [Color figure can be viewed at wileyonlinelibrary.com]

TABLE 1 Radiation pattern characteristics of the proposed microstrip antenna in simulation and fabrication

	Simulation						**Measurement**					
	***xz*-plane**		***yz*-plane**		***xy*-plane**		***xz*-plane**		***yz*-plane**		***xy*-plane**	
Gain	E_θ	E_ϕ	E_θ	E_ϕ	E_θ	E_ϕ	E_θ	E_ϕ	E_θ	E_ϕ	E_θ	E_ϕ
Max. (dBi)	−2.01	−2.19	−2.18	−2	−2.37	−1.63	−3.12	−2.7	−3.24	−3.29	−4.47	−4.08
Min. (dBi)	−4.15	−3.32	−4.79	−3.14	−4.55	−3.5	−5.52	−5.01	−5.3	−4.99	−6.96	−6.8
Difference (dB)	2.14	1.13	2.61	1.14	2.18	1.87	2.4	2.31	2.06	1.7	2.49	2.72

density **M** was made in the same direction. Therefore, a $\lambda/4$ microstrip antenna was designed in which the leakage electric field at the edge of the radiating element contributes to radiation in the same direction, not only from the feed axis but also from the side. Next, the two designed antennas were combined in a "+" shape to feed a microstrip line near the intersection point of the vertically couple antennas. As a result, the E_θ and E_ϕ components showed a nondirectional pattern with a level difference of less than 3 dB between the maximum and minimum values in all directions. These

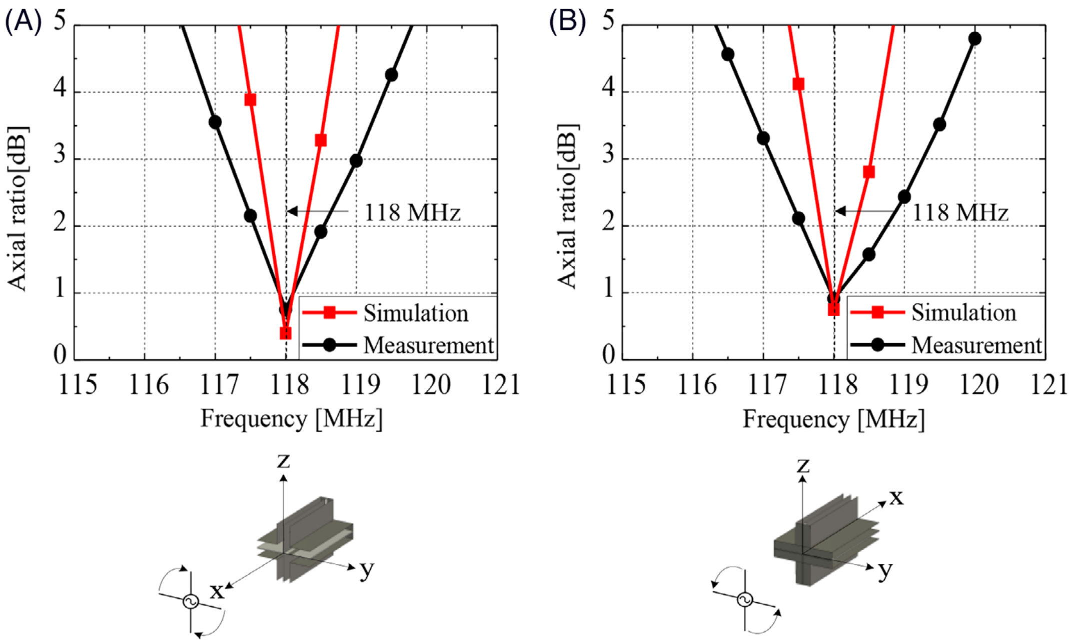

FIGURE 5 Axial ratio of the proposed microstrip antenna: (A) right-handed circular polarization; (B) left-handed circular polarization [Color figure can be viewed at wileyonlinelibrary.com]

results verify that the antenna proposed in this study was isotropic with nondirectional characteristics in all polarization and directional conditions. It can also cover drones and autonomous vehicles and will be useful as antennas for 5G and 6G.

CONFLICT OF INTEREST

The authors declare that they have no conflicts of interest with the contents of this article.

ACKNOWLEDGEMENT

This work was supported by Institute of Information & communications Technology Planning & Evaluation (IITP) grant funded by the Korea government (MSIT) (No. 2021-0-00486, Augmented Beam-routing: Carom-MIMO).

ORCID

Dong-Su Choi https://orcid.org/0000-0002-8951-3261

REFERENCES

[1] Carver KR, Mink JW. Microstrip antenna technology. *IEEE Trans Antennas Propag*. 1981;AP-29:2-24. https://ieeexplore.ieee.org/stamp/stamp.jsp?arnumber=1142523.

[2] James JR, Hall PS, Wood C. *Microstrip Antenna Theory and Design*. London, UK: Peter Peregrinus; 1981. https://digital-library.theiet.org/content/books/ew/pbew012e.

[3] Balanis CA. *Antenna Theory: Analysis and Design*. 2nd ed. Hoboken, NJ: John Wiley & Sons; 2005:771-829.

[4] Bae J-W, Jeon H-S, Kim D-M, Yeom C-H. Ground based augmentation system (GBAS) technology development and construction trend. *Curr Ind Technol Trends Aerosp*. 2011;9:187-195. https://www.dbpia.co.kr/journal/articleDetail?nodeId=NODE01753782.

[5] Bae JW, Yun YS, Choi CH, Jeong MS, Kim DM, Jun HS. A study on the approval process and criteria for operation of ground-based augmentation system (GBAS) in Korea. *J Korean Soc Aviat Aeronaut*. 2014;22:115-125. https://doi.org/10.12985/ksaa.2014.22.4.115.

[6] Heo H-M, Woo J-M. Miniaturization of the microstrip antenna using the folded structure. Paper presented at: Proceedings of Microwave and Propagation Conference, 2004;27:431-434.

[7] Woo J-M, Sim Y-B, Kim Y-R. Multiple polarization folded microstrip antenna. Paper presented at: Proceedings of KIEES Spring Microwave and Propagation Conference, 2006;29:137-140.

[8] Kim M-W, Woo J-M. Omnidirectional microstrip patch antenna. Paper presented at: Proceedings of KIEES Spring Microwave and Propagation Conference, 2015;38:98.

[9] Moon S-M, Ryu H-K, Woo J-M, Ling H. Miniaturisation of /4 microstrip antenna using perturbation effect and plate loading for low-VHF-band applications. *Electronics Letters*. 2011;47:162. https://doi.org/10.1049/el.2010.3647.

[10] Song M-H, Woo J-M. Miniaturisation of microstrip patch antenna using perturbation of radiating slot. *Electronics Letters*. 2003;39:417. https://doi.org/10.1049/el:20030260.

How to cite this article: Choi D-S, Choi Y-S, Ju D-K, Jung BC, Woo J-M. Folded microstrip antenna with isotropic radiation pattern. *Microw Opt Technol Lett*. 2021;1–7. https://doi.org/10.1002/mop.32992